Design and Parallel Synthesis of Novel Selective Hydrogen Oxidation Catalysts and their Application in Alkane Dehydrogenation

L. M. (Lars) van der Zande, E. A. (Bart) de Graaf, Gadi Rothenberg*

Chemical Engineering Department, Universiteit van Amsterdam, Nieuwe Achtergracht 166, 1018 WV Amsterdam, The Netherlands
Fax: (+31)-20-525-5604, e-mail: gadi@science.uva.nl

Received: April 19, 2002; Accepted: June 21, 2002

Supporting information for this article is available on the WWW under http://www.wiley-vch.de/home/asc or from the author.

Abstract: A library of 19 supported metal oxides of group IIIA, IVA, and VA metals is prepared using a simple gram-scale reactor for parallel pore impregnation. The activity, stability, and selectivity of these potential hydrogen combustion catalysts in the dehydrogenation of ethane to ethylene at 600 °C is examined over several redox cycles using gas mixtures that simulate real process conditions. Lead, indium, and thallium oxides are highly selective (>99.9%) to hydrogen combustion. Low-loading catalysts are found to exhibit higher oxygen exchange activity. Differences between co-fed and redox oxidative dehydrogenation are discussed.

Keywords: combinatorial catalysis; gas-solid reactions; heterogeneous catalysis; hydrogen combustion; parallel reactor; solid oxygen carriers

Introduction

The catalytic dehydrogenation of alkanes to alkenes [Equation (1)] is a key step in the industrial production of core synthetic materials. It is a well established commercial process that is running in several large-scale plants.[1] The catalysts commonly used are platinum[2] supported on alumina,[3,4] doped platinum on zeolites,[5a] or various types of chromia on alumina. [5b] There are two main drawbacks, however: (i) reaction thermodynamics dictate low olefin yields (*ca.* 20–40%, depending on reactant and temperature), and (ii) the process is highly endothermic so that expensive energy must be externally supplied.

$$C_nH_{2n+2} \underset{400\text{–}700\ ^\circ C}{\overset{\text{catalyst}}{\rightleftharpoons}} C_nH_{2n} + H_2 \qquad (1)$$

An attractive simultaneous solution to both problems is the use of a redox cycle system that burns the hydrogen product to produce the required energy (Scheme 1). Using hydrogen as fuel is advantageous as the heat is produced on the spot where it is consumed with no heat transfer losses. The elegance and simplicity of this solution has stimulated efforts to investigate potential selective hydrogen oxidation catalysts. Notably, Grasselli and co-workers have recently published several important papers on the principles and process options of such redox systems.[6–11]

One obstacle in the application of this redox cycle is the low selectivity and stability of state-of-the-art hydrogen oxidation catalysts under the conditions required for the dehydrogenation reaction.[12] A second is the obvious hazard arising from the mixing of alkanes, hydrogen, and oxygen at high temperatures. Our approach to solving these problems was to use solid "oxygen reservoirs" that release lattice oxygen atoms from their crystals selectively in the presence of hydro-

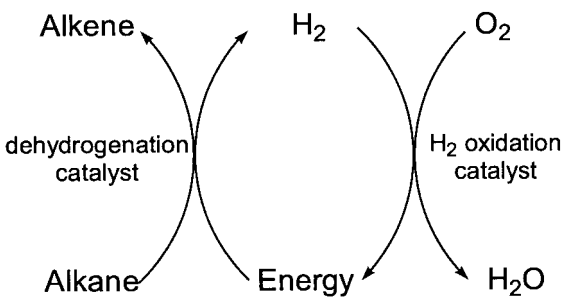

Scheme 1. Redox cycle.

  1615-4150/02/34408-884–889 $ 17.50+.50/0

gen. Preliminary studies showed metal oxides of groups IIIA–VA to be promising candidates as far as selectivity was concerned. However, due to their low specific surface area and low melting point the stability of the pure metal oxides is poor and their activity is quickly diminished by sintering. In this paper, we report the synthesis of 19 group IIIA–VA-supported solid oxygen carriers, and examine their activity, selectivity and stability as hydrogen oxidation catalysts under simulated dehydrogenation process conditions. The catalysts' synthesis was carried out in a simple parallel pore impregnation reactor that was built in-house.

Results and Discussion

Catalyst Library Design and Synthesis

Earlier investigations[11] postulated that the active metal site interacts with the hydrogen molecule through lone pair interactions in its oxide state. The post-transition metals (groups IIIA–VIA) all fulfil this requirement, but some members of this set are either radioactive (Po) or have too low a melting point (Al, Ga, Ge, Sn, *cf.* the reaction temperature 450 – 650 °C) or are too poisonous to be considered (As). This leaves In, Sb, Tl, Pb, and Bi. Using these five metals we synthesised high (1 mmol g^{-1}) and low (0.5 mmol g^{-1}) loading materials on two different supports (alumina and silica). With the exception of Sb, concentrated nitrate salt solutions were employed as catalyst precursors for the pore impregnation process (see experimental section for details).

A serious drawback of the pore impregnation technique is the limited pore volume available for each impregnation step. Moreover, to obtain good dispersion the impregnation is better carried out using several small portions of active material (e.g., up to 10 impregnation steps per sample were required to synthesise the catalysts with 1 mmol g^{-1} loading). Such repetitive experiments are time-consuming and labour intensive. Specifically in the synthesis of heterogeneous catalysts, it is important to keep the preparation parameters as uniform as possible.[13] Similar problems in the preparation of heterogeneous catalysts have been addressed recently, and several ingenious and elegant solutions have been proposed.[14–17] In our case, we required a method to synthesise gram quantities of supported materials in an efficient and reproducible manner. To this end we constructed a lab-scale parallel reactor for pore impregnation (Figure 1). This simple and inexpensive device reduces the time required for catalyst preparation by an order of magnitude and enables the preparation of catalyst batches under identical conditions (please refer to the supporting information for detailed construction and operation parameters). In principle such parallel pore impregnation could also be carried out using commercial multireactor blocks. The apparatus described here, however, is cheaper by two orders of magnitude.

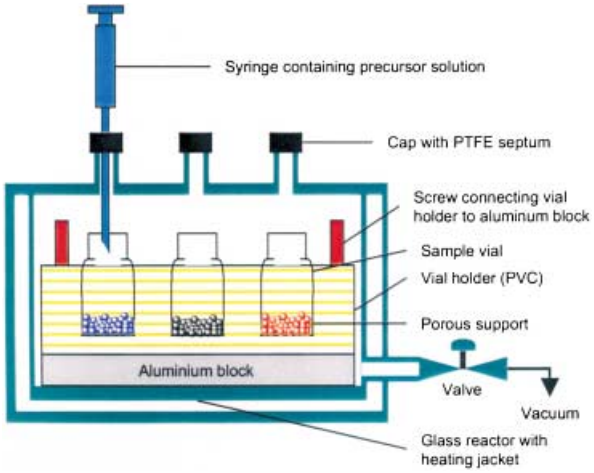

Figure 1. Parallel reactor for pore impregnation in which up to seven samples of 0.1 – 2.0 g material can be prepared simultaneously (for clarity only three vials are shown).

Redox Reaction Cycles

We used a feed stream that simulated the effluent at the end of the dehydrogenation process. Using a cyclic mode of operation, this feed was stripped of its hydrogen by reaction with the solid oxygen carrier, which was subsequently cleaned and regenerated with oxygen (Scheme 2). In this way hazardous contact between the oxygen gas and the hydrogen/hydrocarbon mixtures was avoided.

A typical experiment included ten consecutive four-step cycles of reduction, inert purge, re-oxidation, and inert purge. In the reduction (step 1) a feed consisting of ethane (20% v/v), ethylene (20%), hydrogen (5%), nitrogen (tracer gas, 2%), and helium (inert carrier gas) was flowed through a fixed-bed quartz reactor at a flow rate of 50 mL min^{-1} at 600 °C. Gas effluent samples were taken at regular intervals and analysed by GC. Thereafter, the catalyst bed was purged (step 2) with pure helium. The solid oxygen carrier was then re-oxidised (step 3) using 1% O_2 in helium at a flow rate of 50 mL min^{-1} wherein the effluents were continuously observed by online mass spectrometry. The catalyst bed was purged again with helium (step 4) and this whole cycle was repeated 9 times.

Activity and Stability

Figure 2 shows the mol % of the oxygen atoms that are "extracted" in each cycle for the 19 different catalysts. Catalysts **D** and **M** display surprising activity – in both

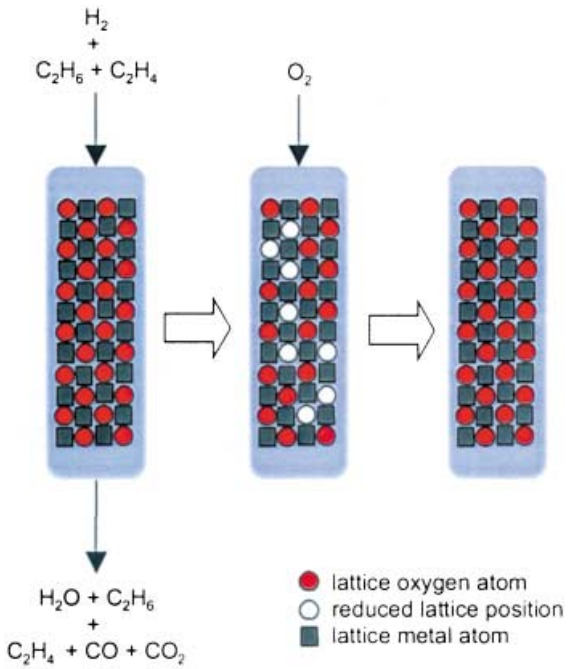

Scheme 2. Cartoon of the reaction set-up showing the selective "extraction" of lattice oxygen atoms in the reduction step and their replacement in the oxidation step (for clarity, an ideal mixing of the solids is assumed, and surface effects and the two purge cycles with He are not shown).

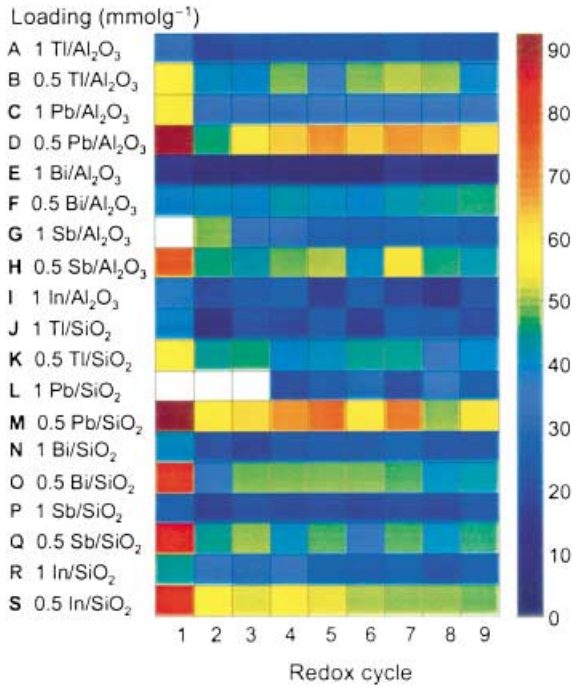

Figure 2. Available oxygen (mol % out of theoretical limit, white = n/a) per redox cycle using group IIIA–VA-supported metal oxides. Cycle conditions: 50 mL min^{-1} constant flow at 600 °C, oxidation (1% O_2 in He for 18 min), purge (pure He for 1 min), reduction (5% H_2, 20% C_2H_6 and 20% C_2H_4 in He for 10 min), and purge (He, 1 min).

cases the active material is a low-loading lead oxide, PbO. In several cases (catalysts **B**, **D**, **H**, **M**, **O**, and **S**) the oxygen consumption is stable at the 50% mark or higher, meaning that more than half of the oxygen atoms in these solid "oxygen reservoirs" are utilised. It could be that 50 – 70% oxygen utilisation is the highest reachable value from a practical viewpoint, as one could expect a "collapse" of the oxide crystal if more oxygen atoms are taken out. The initial decrease in activity observed for practically all of the materials during the first cycle is probably due to sintering that occurs during reduction at temperatures above or close to the melting point of the supported metals. Using either silica or alumina as catalyst support did not afford significant changes in the activity and stability. All the following discussion pertains to cycles 4 – 9, where the materials remain stable.

While the fraction of available lattice oxygen atoms is of interest for structure-activity studies, the total amount of oxygen available *per gram material* (i.e., the specific oxygen storage capacity of the catalyst) is the key parameter from the industrial perspective. As shown in Figure 3 for 0.5 mmol g^{-1} loading as well as for 1 mmol g^{-1} loading(data not shown) the amount of available oxygen does not differ much between low and high metal loadings (*cf.* the continuous and the broken lines in Figure 3). This is remarkable, for one could expect that doubling the loading from 0.5 mmol g^{-1} to 1 mmol g^{-1} would result in a significant change in capacity.

Three factors can account for this observation: first, these are heavy metals and the weight of the supported material itself is not negligible at 1 mmol g^{-1} loadings. (The wt % of the supported material for 1 mmol g^{-1} metal oxide loading is 23.3%, 22.8%, 22.3%, 14.6%, and 13.9% for Bi, Tl, Pb, Sb, and In, respectively.) Second, sintering can occur under the combination of reduction and high temperature. After the first cycle, the reduced metal aggregates may sinter to form larger particles. Although in subsequent oxidation cycles all of the metal atoms are re-oxidised, the high initial dispersion would not be regained. Third, some of the metals can vaporise at these high temperatures. In the case of Bi, Sb, In, and Tl coloured bands were observed in the lower part of the reactor tube. It is likely that a fraction of the metal is vaporised at 600 °C and condenses at the exit of the reactor, where the temperature is only 120 °C.

Selectivity

Two-step oxidative dehydrogenation must exhibit excellent selectivity towards hydrogen oxidation if it is to compete with industrial dehydrogenation processes.

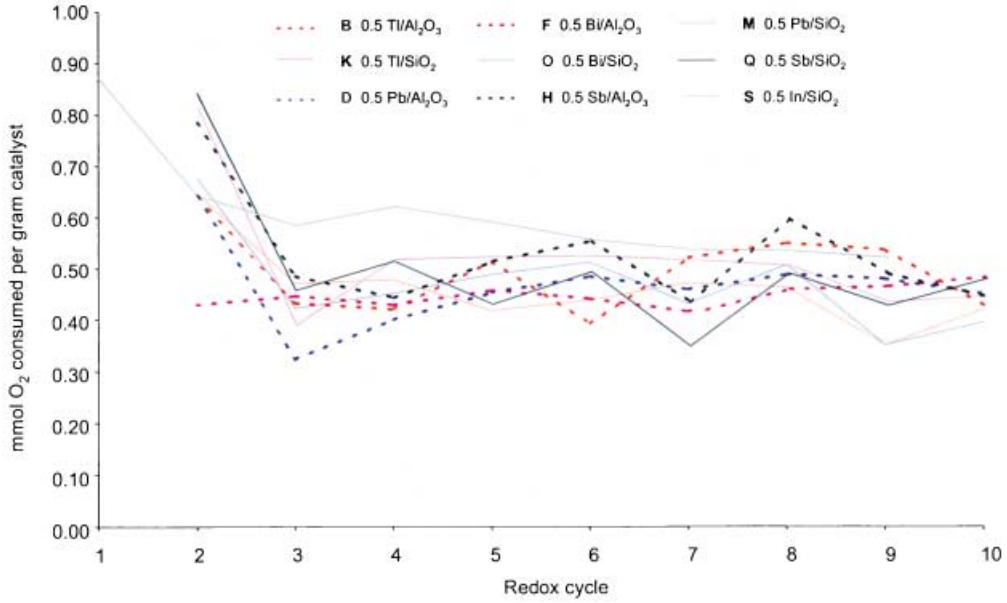

Figure 3. Consumption of oxygen per gram catalyst over 10 redox cycles. Silica-supported materials shown by continuous lines and alumina-supported by broken lines. All catalysts contain 0.5 mmol g^{-1} active material, conditions are the same as in Figure 2.

Otherwise the additional separation steps would render it uneconomical. The selectivity of catalysts **A**–**S** towards hydrogen oxidation in the presence of ethane and ethylene is shown in Table 1. In most cases, only the last 6 redox cycles were taken into account, as this was the region where the materials exhibited stable behaviour (*cf.* Figure 3). In all cases the selectivity was good (> 99.5%) and only minor amounts of CO and CO_2 were observed. Traces of CH_4 were also observed in some cases, but the amount was at instrumental detection

Table 1. Catalyst selectivity in the combustion of hydrogen.[a]

Entry	Catalyst (loading m molg^{-1})	Support	Selectivity, % ($\pm$0.1%)[b, c]
1	**D** PbO (0.5)	Alumina	> 99.9
2	**J** Tl_2O_3 (1)	Silica	> 99.9
3	**L** PbO (1)	Silica	> 99.9
4	**O** Bi_2O_3 (0.5)	Silica	> 99.9
5	**Q** Sb_2O_3 (0.5)	Silica	> 99.9
6	**S** In_2O_3 (0.5)	Silica	> 99.9
7	**A** Tl_2O_3 (1)	Alumina	> 99.9
8	**B** Tl_2O_3 (0.5)	Alumina	> 99.9
9	**R** In_2O_3 (1)	Silica	> 99.9
10	**M** PbO (0.5)	Silica	99.9
11	**C** PbO (1)	Alumina	99.9
12	**F** Bi_2O_3 (0.5)	Alumina	99.8
13	**G** Sb_2O_3 (1)	Alumina	99.8
14	**H** Sb_2O_3 (0.5)	Alumina	99.8
15	**I** In_2O_3 (1)	Alumina	99.8
16	**P** Sb_2O_3 (1)	Silica	99.8
17	**K** Tl_2O_3 (0.5)	Silica	99.8
18	**E** Bi_2O_3 (1)	Alumina	99.7

[a] Reaction conditions: 50 mg catalyst sample, 600 °C, 10 redox cycles [50 mL min^{-1} constant flow at 600 °C, oxidation (1% O_2 in He for 18 min), purge (pure He for 1 min), reduction (5% H_2, 20% C_2H_6 and 20% C_2H_4 in He for 10 min), and purge (He, 1 min)].

[b] Calculated by dividing the total amount of deep oxidation products ($CO + CO_2$, based on GC area corrected by the presence of an internal standard) by the total O_2 consumption as determined by mass spectrometry.

[c] The values shown are an average over the last 6 redox cycles only, as this is the region where all catalysts showed stable behaviour. The measurement error is $\pm$ 0.1%.

level. Catalysts **A**, **B**, **D**, **J**, **L**, **O**, **Q**, **R**, and **S** showed excellent selectivity towards H_2 combustion (>99.9%) with other products being on the instrumental detection limit. In general, catalysts supported on silica tended to be more selective than those supported on alumina.

An exact quantitative comparison between these catalysts and those reported earlier cannot be performed because the experimental conditions vary between the studies (previous studies were performed in co-fed mode, i.e., the O_2 and the H_2/HC's mixture were fed into the reactor simultaneously). However, comparing our results to those reported by Grasselli shows that in both cases Tl, Sb, and In exhibited good selectivity. Again, the performance of the lead oxides is remarkable, especially as previous reports showed lower selectivities for lead.[9] These differences might be due to changes in selectivity as a function of the degree of reduction[18] or to changes in the lead oxide itself as a result of the different temperatures (lead oxide changes from Pb_3O_4 to PbO at around 500 °C).

Further studies are required to establish the oxidation mechanism. At this stage it is possible only to distinguish the fundamental differences between redox and co-fed oxidative dehydrogenation modes. In co-fed mode, the metal oxide oxygen is constantly being replenished so that the most active oxygen atoms (i.e., those forming the overlayer of the metal oxide crystal[19]) would play a major role in the reaction. Conversely, in redox mode bulk oxygen atoms and subsurface oxygen have to be activated (*cf.* Figure 2 where the oxygen utilisation is ~50 mol %). This can be achieved either by diffusion of O^{2-} ions from the bulk to the surface or perhaps by diffusion of hydrogen into the oxide lattice (diffusion of ethane or ethylene into the lattice is extremely unlikely). Hydrogen is a stronger reducing agent than either ethane or ethylene and may be able to reduce subsurface oxygen atoms. Also, oxygen atoms situated directly on the surface (overlayer atoms) should be equally available to both hydrogen and hydrocarbon molecules, while atoms from lower layers would less accessible to the hydrocarbons.

Conclusion

Parallel pore impregnation is an effective method for the synthesis of supported catalyst libraries on a gram scale. Supported oxides of group IIIA–VA metals display good activity, good stability and high selectivity towards hydrogen oxidation in redox mode under simulated dehydrogenation conditions. The combination of these materials with a suitable dehydrogenation catalyst either *in* or *ex situ* may provide a practicable approach to selective oxidative dehydrogenation. The mechanism by which the lattice oxygen atoms are reduced is yet to be deciphered and is currently under investigation in our laboratory.

Experimental Section

General Remarks

GC analysis was performed at 50 °C on a Carlo Erba 4300 instrument modified with a 16-way valve to enable fast sampling and a 3 m Alltech Unibead 1S column, using 1 mL min^{-1} N_2 (99.5%, Hoekloos) as internal standard. MS analysis was performed using a Pfeiffer QMA 200 instrument (*m/z* range 0–100). Unless noted otherwise, all chemicals were purchased from commercial firms and used as received. Supported metal oxides were prepared from the corresponding metal nitrate precursors, except in the case of Sb where the tartarate complex was used. Ketjen CK300 alumina (surface area 208 m^2 g^{-1}, pore volume 0.68 mL g^{-1}) was ground, sieved to 60 - 80 mesh size, dried for 24 h and then re-hydrated for 24 h in air at 25 °C before use. Grace 121 silica (surface area 670 m^2 g^{-1}, pore volume 0.351 mL g^{-1}) was used as received. C_2H_4 (99.7% pure), He (99.996%), O_2 (99.5%, dried over molecular sieves before use), and H_2 (99.999%, purified by a BTS column and dried over molecular sieves before use) were purchased from Praxair. C_2H_6 (99.3%) was purchased from Ucar. All gas streams were dried using a Perma Pure MD-050-72S membrane prior to GC analysis. The order of experiments was randomised to minimise systematic error.

General Procedure for Cyclic Redox Experiments

The catalyst sample (50 mg) was mounted on quartz wool in a quartz tube reactor (4 mm inner diameter) and heated to 600 °C under He (50 mL min^{-1}). The reactor temperature was maintained at 600 °C and the sample was subjected to a constant flow of 50 mL min^{-1} of 1% O_2 (v/v) in He for 18 min. The reactor was then purged with He for 1 min, subjected to a reducing mixture of 5% H_2, 20% C_2H_6, and 20% C_2H_4 in He for 10 min, and purged again with He for 1 min. This cycle was repeated 10 times. The product streams were analysed by MS and GC, enabling the determination of H_2, N_2, O_2, CO, CH_4, C_2H_4, C_2H_6, and CO_2, in this order.

General Procedure for Preparation of Supported Catalysts

Example of 0.5 mmol g^{-1} Pb on alumina: $Pb(NO_3)_2$ (0.5 mmol, 5.26 g) was dissolved in demineralised water (19.37 g). Alumina (1.00 g) was placed in a glass vial in the impregnation reactor. The reactor was evacuated and 0.61 mL solution was injected using a syringe. The reactor was vehemently shaken for 4 min using a vortex instrument. The material was dried overnight at 120 °C and exposed to air for 24 h at 25 °C. A second impregnation was carried out (0.10 mL of the solution is diluted with 0.64 mL demineralised water, 0.61 mL of this mixture is injected), the material was dried again overnight and then calcined in ceramic vessels at 650 °C for 5 h (heating rate 300 °C/h) under a flow of dry air (125 mL min^{-1}). Typical yields were over 1.2 g material, an amount sufficient for more than 20 experiments.

Other catalyst samples were similarly prepared, using up to 9 impregnation cycles per sample (depending on the solubility of the precursor salts in water).

Supporting Information Available

Description and photo of the parallel pore impregnation reactor; synthesis procedure for the antimony tartarate complex.

Acknowledgements

We thank Mr. A. Andreini for instructive discussions on pore impregnation mechanisms, Dr. J. A. Westerhuis for advice on experimental design and Mrs. M. Mittelmeijer-Hazeleger for performing the support surface characterisation.

References and Notes

[1] M. P. Atkins, G. R. Evans, *Ber. - Dtsch. Wiss. Ges. Erdoel, Erdgas Kohle, Tagungsber.* **1993**, *9305*, 201.
[2] B. V. Vora, P. R. Pujado, R. F. Anderson, *Energy Prog.* **1986**, *6*, 171.
[3] Y. Ando, X. Li, E. Ito, M. Yamashita, Y. Saito, *Stud. Surf. Sci. Catal.* **1993**, *77*, 313.
[4] P. A. Van Trimpont, G. B. Marin, G. F. Froment, *Ind. Eng. Chem. Fundam.* **1986**, *25*, 544.
[5] a) X.-K. Wang, S.-Y. Peng, *J. Nat. Gas Chem.* **1994**, *3*, 353; b) B. M. Weckhuysen, R. A. Schoonheydt, *Catalysis Today* **1999**, *51*, 223.
[6] P. A. Agaskar, R. K. Grasselli, J. N. Michaels, P. T. Reischman, D. L. Stern, J. G. Tsikoyiannis, *US Patent* 5,563,314, **1996**; *Chem. Abstr. 125*, 300454.
[7] P. A. Agaskar, R. K. Grasselli, J. N. Michaels, P. T. Reischman, D. L. Stern, J. G. Tsikoyiannis, *US Patent* 5,527,979, (Mobil Oil Corporation, USA), **1996**; *Chem. Abstr.* **125**, 142094.
[8] R. K. Grasselli, D. L. Stern, J. G. Tsikoyiannis, *Appl. Catal., A* **1999**, *189*, 9.
[9] R. K. Grasselli, D. L. Stern, J. G. Tsikoyiannis, *Appl. Catal., A* **1999**, *189*, 1.
[10] R. K. Grasselli, D. L. Stern, J. G. Tsikoyiannis, *Stud. Surf. Sci. Catal.* **2000**, 130A, 773.
[11] J. G. Tsikoyiannis, D. L. Stern, R. K. Grasselli, *J. Catal.* **1999**, *184*, 77.
[12] L. Late, J. I. Rundereim, E. A. Blekkan, *Stud. Surf. Sci. Catal.* **2001**, *136*, 289.
[13] R. Schlögl, *Angew. Chem. Int. Ed.* **1998**, *37*, 2333.
[14] S. Senkan, *Angew. Chem. Int. Ed.* **2001**, *40*, 312.
[15] A. Holzwarth, P. Denton, H. Zanthoff, C. Mirodatos, *Catalysis Today* **2001**, *67*, 309.
[16] U. Rodemerck, D. Wolf, O. V. Buyevskaya, P. Claus, S. Senkan, M. Baerns, *Chem. Eng. J.* **2001**, *82*, 3.
[17] B. Jandeleit, D. J. Schaefer, T. S. Powers, H. W. Turner, W. H. Weinberg, *Angew. Chem. Int. Ed.* **1999**, *38*, 2495.
[18] P. Pantu, K. Kim, G. R. Gavalas, *Appl. Catal. A - Gen.* **2000**, *193*, 203.
[19] F. H. M. Dekker, G. Klopper, A. Bliek, F. Kapteijn, J. A. Moulijn, *Chem. Eng. Sci.* **1994**, *49*, 4375.